Influence of Adipose-Derived Mesenchymal Stromal Cell Demineralized Bone Composite on New Bone Formation in Critical Sized Cortical Bone Defects

Nicole P Ehrhart, Laura Chubb, Elissa Flaumenhaft, Carolyn Barret, Yaling Shi

Abstract:

The relatively recent discovery that MSCs derived from various tissues will differentiate into osteoblasts in the presence of osteopromotive medium has allowed for new therapeutic opportunities in bone tissue engineering. We recently described the *in vitro* characteristics of a demineralized bone scaffold containing adipose-derived mesenchymal stromal cells (DBM/hMSC) harvested from human adipose tissue and demonstrated that this combination contains the three components that are considered optimal for bone repair: an osteoconductive scaffold, osteoinductive signaling proteins and osteogenic cells. The objective of this study was to compare and characterize the *in vivo* bone- forming activity of DBM/hMSC to that of DBM alone, hMSCs alone, cortico-cancellous isograft and human cortico-cancellous xenograft in an athymic rat model. A series of animal experiments were performed comparing new bone formation in critical-sized bone defects implanted with DBM/hMSC, DBM, hMSC, corticocancellous isograft, human cortico-cancellous bone graft or no treatment (empty defect). New bone formation was greatest in bone defects implanted with DBM/hMSC when compared with DBM alone, hMSCs alone, corticocancellous bone isograft, or human corticocancellous bone graft. Together, these data support preclinical proof-of-concept that DBM/hMSC will enhance bone formation in challenging healing environments.

1. Introduction

The use of autologous cortico-cancellous bone graft (autograft) is considered the 'gold standard' for bone regeneration and contains three components that are considered to be essential for bone grafting: an osteoconductive scaffold, osteo-inductive signaling proteins and osteogenic cells. Many bone graft substitutes (BGS), such as synthetic ceramics or newer BGS containing recombinant human BMP-2 (Infuse®) lack all three of these components. One commonly utilized BGS, human demineralized bone (DBM), is closely related to autologous bone in terms of composition and function, although it lacks a cellular component.

There is substantial evidence in the scientific literature demonstrating that culture-expanded MSCs derived from various tissues will differentiate into osteoblasts in the presence of osteopromotive medium.[1-4] Moreover, investigators have demonstrated bone formation *in vivo* utilizing culture-expanded MSCs that were exposed to osteopromotive medium *ex vivo* prior to implantation.[5, 6] Because *ex vivo* expansion of MSCs may require weeks and poses certain questions regarding safety[7, 8], a readily available source of MSCs that could be utilized for bone regeneration that does not require expansion is desirable.

We recently demonstrated that a demineralized bone scaffold containing MSCs (DBM/hMSC) harvested from human adipose tissue contains the three components that are considered optimal for bone repair.[9] This study characterized both the cellular and scaffold components, although the characterization was limited to *in vitro* testing. To further explore the bone-forming activity of the DBM/hMSC combination, we completed a series of proof-of-concept *in vivo* studies, utilizing adipose-derived MSCs obtained from human tissue donors, without culture expansion or pre-differentiation. The objective of the series of preclinical experiments reported herein was to compare and characterize the *in vivo* bone forming activity of DBM/hMSC to that of DBM alone, hMSCs alone, cortico-cancellous isograft (derived from rat) and human cortico-cancellous xenograft.

2. Materials and Methods

2.1 hMSC Preparation

Human tissue donors with consent for research use were utilized for the purposes of the study. Adipose tissue was sterilely harvested from deceased human tissue donors and processed using previously published techniques [9] to obtain the stromal vascular fraction (SVF). SVF and growth medium (DMEM/F-12, Corning, Manassas, VA) were combined 1:1 (v/v) in a culture flask and incubated at 37°C with 5% CO_2, Passage 2 cells were obtained and were frozen in 10% DMSO + 90% FBS in the liquid nitrogen vapor phase until needed for either implantation or seeding.

2.2 DBM Preparation

Morselized human cancellous (1-2mm diameter) and cortical bone (1-2mm diameter) was demineralized for 60 minutes in 1 N HCl, neutralized with sterile water and phosphate buffered saline (PBS), and then tested for calcium content by inductively coupled plasma spectroscopy analysis (SunLabs, Tampa, FL) until testing confirmed calcium content of less than eight percent (per AATB standards). The final ratio of cancellous to cortical demineralized bone was 8:2 v/v. DBM was stored at room temperature until needed for implantation or seeding.

2.3 DBM/hMSC Preparation

hMSC and DBM from the same human donor were prepared as described above. Using proprietary conditions, the cancellous DBM was incubated with the SVF to allow attachment of cells followed by a washing procedure. The resulting DBM/hMSC containing approximately 50,000 hMSC/cc of DBM was placed into cryopreservation medium (10% DMSO, 90% FBS) and stored frozen at -80ºC until implantation.

2.4 Human Cortico Cancellous Bone Graft Preparation

Cortico-cancellous bone graft material was harvested from human tissue donors and was placed

in cryopreservation medium (10% DMSO, 90% serum) and stored at -80°C for 72 hours prior to implantation

2.5 Rat Cortico-Cancellous Bone Graft Preparation

Three 12 week old male athymic (RNU/RNU) rats were obtained from Harlan Laboratories and used for bone graft donors. Rats were humanely euthanized and the humeri and femurs were sterilely harvested. The distal and proximal one third of each bone was stripped of soft tissues. The cortical and cancellous bone was morselized into 1-2 mm diameter pieces. The resulting morsels were rinsed in sterile physiologic saline, placed in cryopreservation medium (10% DMSO, 90% serum) and stored at -80°C for 72 hours prior to implantation.

2.6 In Vivo Experiments

A series of four *in-vivo* experiments were performed to characterize the bone-forming properties of DBM/hMSC and its component parts: 1) an intramuscular osteoinductive assay, 2) an acute critical size bone defect study, 3) a chronic critical-size bone defect study, and 4) a comparison study of DBM/hMSC with rat and human corticocancellous bone graft in a critical sized bone defect. All in vivo experiments were performed in compliance with the U.S. Department of Agriculture's (USDA) Animal Welfare Act (9 CFR Parts 1, 2, and 3) and the NIH Guide for the Care and Use of Laboratory Animals and received IACUC approval.

2.7 Intramuscular Osteoinduction Assay

Six 11 week old athymic male rats were used for the study. Four rats were randomly assigned to receive DBM/hMSC and two rats received hMSCs only. Under sterile conditions, an intramuscular pocket was surgically created between the adductor brevis and the semi-membranosis muscles in each hind limb. In eight limbs 0.2 cc of DBM/hMSC containing 50,000 hMSC/cc was implanted. In four limbs, 50,000 MSCs/cc in 0.2 cc of physiologic saline were implanted. Four DBM/hMSC and two hMSC treated limbs were harvested at 14 and at 28 days and the implant sites were collected for histological examination. Harvested tissues were fixed in 10% neutral buffered formalin. Samples were processed in paraffin, cut at 4-6 micrometers and mounted on glass slides. Ten sections per implant were stained with hematoxylin and eosin. A blinded pathologist provided a description of observed elements of new bone formation within each harvested implant site. In addition, each harvested implant was given a yes/ no score for osteoinductivity.

2.8 Acute Critical Sized Bone Defect Feasibility Experiment

Twelve 12 week male athymic (RNU/RNU) rats were obtained from Harlan Laboratories. Under sterile conditions, a custom poly-ethyl-ethyl-ketone (PEEK) plate designed for the study was fixed to the bone using two threaded 0.45 inch diameter K-wires, two on each side of the proposed defect. Following plate fixation, a 5mm defect was surgically created in the right femur using a gigli wire. The rats were randomly assigned to receive one of four treatments. Three rats received 0.5 cc of DBM/hMSC (50,000 hMSC/cc) placed in the bone defect at the time of surgery (DBM/hMSC group). Three rats received 0.5 cc DBM (DBM group). Three rats received 0.5 cc of 50,0000 hMSC/cc 0.9% physiologic saline (hMSC group) placed in the defect. Three rats received no treatment in the defect. The muscles were closed around the plate and defect to contain the implanted material and skin and subcutaneous tissues were closed in routine three layer fashion. Analgesic medications were administered for 72 hours following surgery or longer if the animals exhibited pain or lameness. Animals were observed daily for illness, lameness, swelling or pain.

Radiographs and Quantitative Radiographic Analysis: Radiographs were performed using a high detail digital radiography unit at times 0, 21, and 42 days post-surgery. Implants were evaluated for alignment, adequacy of fixation and positioning. The amount of mineralized tissue that was within the defect was evaluated. At 42 days post-surgery, animals were sacrificed. Operated limbs were harvested and microCT (µCT) analysis followed by histology was performed to evaluate the tissue within the defect. Using digital analysis software, radiographic new bone area was calculated at each time point by an observer blinded to treatment group

3

by outlining mineralized tissue within the defect of each limb at each post-operative time point and calculating mineralized tissue area. Results were reported as mean new bone area per time point.

MicroCT Imaging and Analysis: Following euthanasia, whole femur specimens were harvested. Fixation components were removed and the femurs were placed in 10% neutral buffered formalin until scanning. Femurs were scanned using a µCT-80 imaging system (Scanco USA, Southeastern, PA) at a voxel size of 10 µm to image bone. From the two-dimensional slice images generated, an appropriate threshold was chosen for the bone voxels by visually matching thresholded areas to gray-scale images. The threshold and the volume of interest (VOI) covering the entire length of the defect and 50 slices on each side of the defect were kept constant throughout the analysis for each femur. New bone volume in the volume of interest (VOI) covering the entire length of the defect and the 50 slices of cortical bone at both ends of the defect were used as a quantitative measure of new bone volume.

Tissue Preparation and Histologic Analysis: Following µCT, femurs were decalcified, sectioned and paraffin-embedded in standard fashion for histology. Paraffin blocks were sectioned on the microtome such that 5mm longitudinal sections of the tissue within the defect and approximately 2 mm of cortical bone on the proximal and distal ends of the defect were identifiable on slides for evaluation. Qualitative histological descriptions of the tissues present within the defect were provided for each sample. The degree of inflammation was scored for each sample with 0= none, 1= mild, 2= moderate and 3= severe. The mean inflammatory score for each treatment group was reported.

2.9 Chronic Critical Sized Bone Defect Feasibility Experiment

Twelve 12 week male athymic (RNU/RNU) rats were obtained from Harlan Laboratories and had a 5mm defect created in the femur in an identical manner as in the previous experiment. Rats were assigned to the following treatment groups: DBM/hMSC (n=3),; DBM (n=3); hMSC (n=3), [50,000 hMSC/cc in 0.5cc; and no treatment (n=3). Radiographs were obtained at 0,3,6,9 and 12 weeks.

A radiographic union score (Table 1) was assigned for each subject at each timepoint by a reviewer blinded to treatment group. Animals were sacrificed at 12 weeks and operated limbs were harvested for µCT analysis. For this study, samples were scanned on a µCT40 imaging system (Scanco Medical, Zurich, CH) at a 15 µm voxel resolution.. Following µCT, operated femurs were placed in 10% neutral buffered saline. Hematoxylin and eosin stained sections were prepared for histological analysis and examined by a veterinary pathologist. Qualitative histological descriptions were provided for each treatment group.

2.10 Comparison with Rat and Human Cortico-
     cancellous Bone Graft

Nine 12 week male athymic (RNU/RNU) rats were obtained from Harlan Laboratories and had a 5mm defect created in the femur in an identical manner as in the previous experiments. Rats were assigned to the following treatment groups: 0.5 cc DBM/hMSC (n=3), 0.5cc rat-derived fresh frozen corticocancellous bone allograft (n=3), 0.5cc human fresh frozen corticocancellous bone graft (n=3) and no treatment (n=3).

Radiographs and Radiographic Analysis: Radiographs were performed using a high detail digital radiography unit at times 0, 21, and 42 days post-surgery to assess implant integrity, alignment and union. At 42 days post-surgery, study subjects were sacrificed. MicroCT analysis followed by histology was performed on the operated femurs. . The presence or absence of radiographic union was assessed at 42 days by a reviewer blinded to treatment group. µCT analysis was performed as described in the previous experiments.

Tissue Preparation and Histologic Analysis: Following µCT, femurs were decalcified, sectioned and paraffin-embedded as described in the previous sections. Each specimen slide was analyzed using BioQuant Osteo software (Nashville, TN) and the percentage of new bone within the defect area was calculated.

3. Results

All animals survived the in-life phases of the in vivo studies. No systemic illness or surgical site infection in any animal was noted. All rats were ambulating

4

normally by day 6 post-operative and had normal activity and behavior throughout the studies.

3.1 Intramuscular Osteoinduction Assay

At both 14 and 28 days, histological analysis revealed the presence of osteoinduction (osteoinduction score =yes) in 3/3 DBM-treated, in 3/3 DBM/hMSC-treated rats and in 0/3 rats treated with hMSCs alone. Chondroblasts, chondrocytes, osteoblasts, osteocytes, cartilage, osteoid, residual demineralized bone and new bone were noted in all groups at all time points except the hMSC-treated groups. Bone marrow elements were noted at the 28 day time points in the DBM/hMSC-treated groups but not in any other treatment group.

3.2 Acute Critical Sized Bone Defect Experiment

Radiographic Analysis: Appropriate alignment and fixation were maintained throughout the study term. New bone area (mineralized tissue) within the defect increased between day 21 and day 42 post-operative in all groups except the empty defect group. The rats treated with DBM/hMSC had the greatest mean new bone area by 42 days. The no treatment group showed no new mineralized tissue within the defect throughout the study period. Mean new bone area at

day 21 post-operative was 0 cm^2 for the empty defect group, 0.0266 cm^2 for the cells-only group, 0.3754 cm^2 for the DBM group and 0.3030 cm^2 for the DBM/hMSC group. At day 42 post-operative the mean new bone area results were: empty defect = 0 cm^2, hMSC (cells only) =0.1017 cm^2, DBM only= 0.5809 cm^2, and DBM/hMSC 0.8147 cm^2. These data are summarized in Figure 1.

MicroCT Analysis: Mean new bone volume as calculated on μCT showed a similar pattern as new bone area on radiographs. Mean new bone volume within the defects was as follows for each treatment group: no treatment = 0.098 mm^3, cells only = 12.358 mm^3, DBM= 32.821 mm^3 and DBM/hMSC 65.565 mm^3. These data are summarized in Figure 2A. Representative μCT images are shown in Figure 2B.

Histologic Analysis:
No Treatment (Empty Defect)

No bone formation was observed within histological sections of the empty defect group validating the 5 mm defect as a critical size defect in this experiment. Some active fibroplasia was observed with muscle collapse into the defect in two of the three
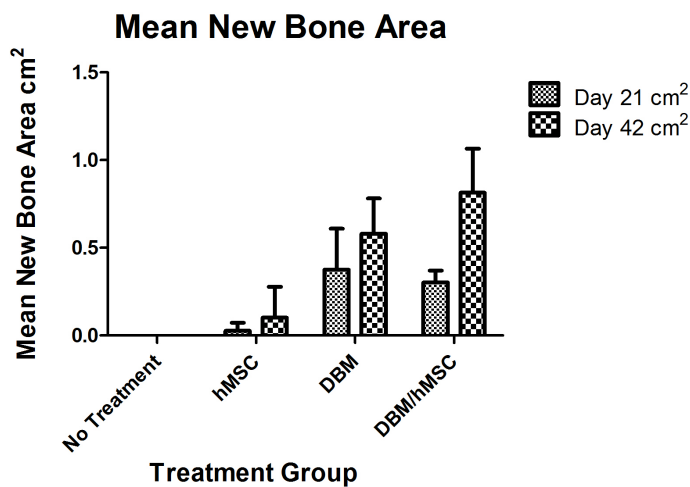

Mean New Bone Area

Figure 1 (left):
Mean new bone area within the critical sized femur defect as determined on digital radiographic analysis at 21 days and 42 days post implantation.
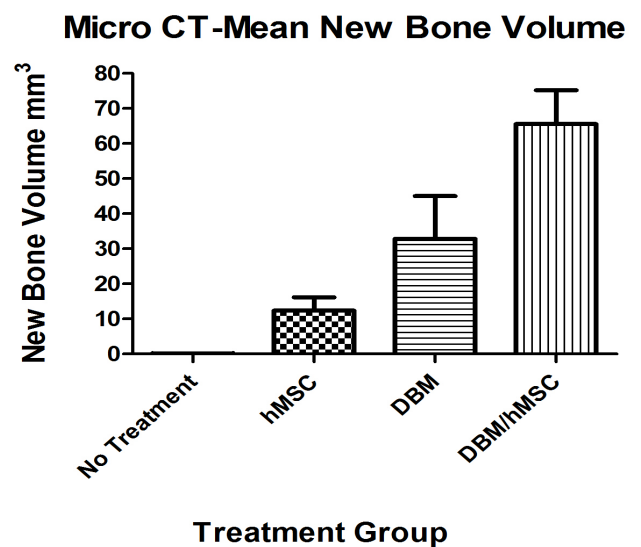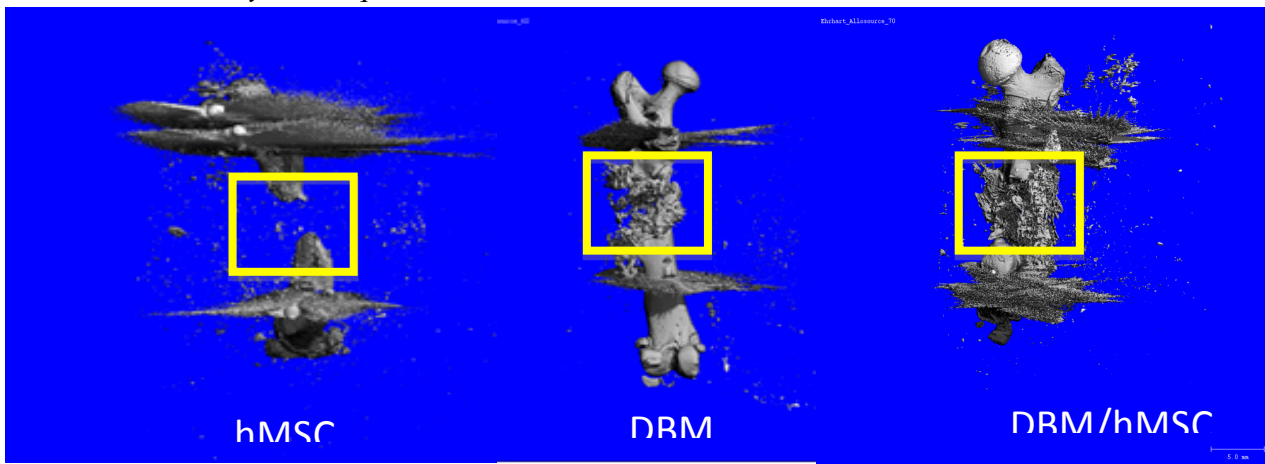

Micro CT-Mean New Bone Volume

Figure 2A (Right):
Mean bone volume within the critical-sized femur defect as determined by μ CT imaging at 42 days post implantation.

Figure 2B (below): MicroCT images of representative samples from defects treated with hMSCs alone, DBM carrier alone and DBM/hMSC. Area of defect is outlined within the yellow square.

all sections evaluated for this treatment. Active fibroplasia was observed in the interstices of the bone chips with fibroblasts producing a very loose, web-like highly vascularized fibrous tissue. Small amounts of osteoblastic bone formation

sections evaluated for this treatment. Inflammation, if observed, was mild and consisted of multinucleated giant cells associated with suture material or degenerate muscle fibers. No marrow components were observed. The mean inflammatory score was 1.

hMSC Group

In defects treated with hMSCs only, fibroplasia was observed with fibrous tissue sometimes spanning the entire length of the defect. Fibrous tissue was of moderate collagen density. Vascularity was observed within the fibrous tissue in these defects. A small amount of osteoblastic bone formation was observed, but it appeared to be associated with host bone rather than the treatment. Inflammation, if observed, was mild and consisted of multinucleated giant cells associated with suture material or degenerate muscle fibers. No marrow components were observed. The mean inflammatory score was 1. Representative histological section is shown in Figure 3A.

DBM Group

In defects treated with DBM carrier only, remaining demineralized bone was visible within

were observed on the surface of the DBM. This was variable between sections and section orientation/placement. Inflammation, if observed, was mild and consisted of multinucleated giant cells associated with degenerate muscle fibers. Some multinucleated cells were visible on the surface of the DBM carrier, indicating ongoing cell-mediated phagocy-tosis/resorption of the demineralized surface. Marrow components were observed within small pockets of the fibrous tissue within the defect adjacent to the host bone. The mean inflammatory score was 1. Representative histological section is shown in Figure 3B.

DBM/hMSC Group

In defects treated with DBM carrier + cells, demineralized bone chips were visible within all sections evaluated. Active fibroplasia was observed in the interstices of the bone chips with fibroblasts producing a loose, highly vascularized fibrous tissue with tissue having a higher collagen density compared to defects treated with DBM alone.

Osteoblastic bone formation was observed most often for this treatment, compared to other treatments, with well- integrated new bone apposed directly to the surface of the DBM. Cartilage cells were present within the defect in all sections evaluated for this treatment. Inflammation, if observed, was mild and consisted

of multinucleated giant cells associated with suture material. Some multinucleated cells were visible on the surface of the DBM carrier likely representing ongoing cell mediated phagocytosis/ resorption of the demineralized surface. Marrow components were observed within small pockets of the fibrous tissue within the defect and adjacent to the host bone. The mean inflammatory score was 1. Representative histological section is shown in Figure 3C.

3.3   Chronic Critical Sized Bone Defect Study

One additional animal was added to the DBM/hMSC group because one of the original subjects had incomplete bi-cortical purchase of a fixation wire used to secure the plate to the femur. Despite concern that the fixation may fail in this animal, the femur remained well aligned throughout the study period and the animal was left on study. Appropriate alignment and fixation were maintained throughout the study term in all animals.
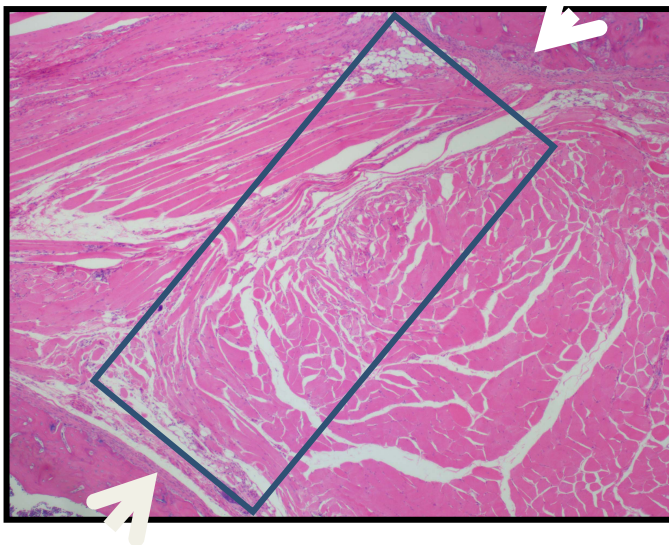

Figure 3A (left): 5X histologic section from the hMSC treatment group. Tissue within rectangle is the area of the defect consisting of normal host muscle and fatty tissue. White arrows show proximal and distal ends of host bone on each side of the defect-.   Note the absence of bone formation.

Figure 3B (below): 10x photomicrograph of DBM treated defect showing new bone formation (black arrows) on DBM (grey arrows)
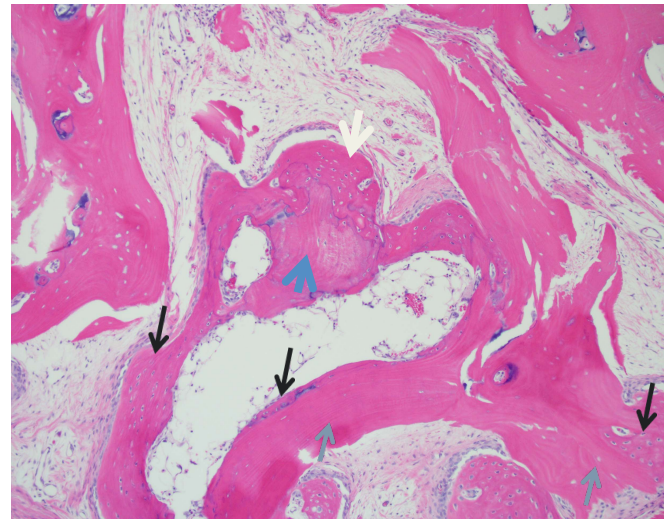
Radiographic Analysis:

The empty defect (no treatment) showed scant evidence of new bone formation (mean radiographic score=0.67). No unions were noted in the empty defect group, validating the 5 mm defect as a critical defect this experiment. The hMSC treatment group showed
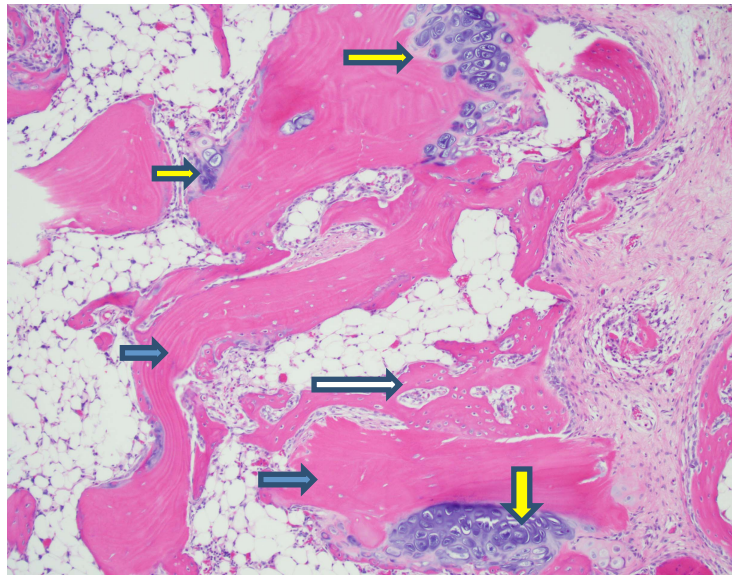
Figure 3C: 10x photomicrograph of DBM/hMSC -treated defect showing new bone formation with marrow components (white arrow) on DBM (grey arrows) and cartilage components (yellow arrows)

scant evidence of new bone formation (median radiographic score=0.67) and had a similar radiographic appearance to the empty defect group. No union was noted in this group. The DBM treatment group had more bone present on radiographs than empty defects or defects treated with hMSC (mean radiograph score =1.33) with one defect progressing to union by day 63. However by 84 days the quality of the union declined and developed radiolucent foci. At day 84, this individual was considered to have an incomplete union.

The hMSC/ DBM treatment demonstrated moderate to robust new bone growth (mean radiographic score = 1.5). These animals demonstrated unions in two of four animals and the bone quality of the unions was maintained throughout the study term.

Figure 4 (right):
Mean bone volume within the critical-sized femur defect as determined by µ CT imaging at 84 days (12 weeks) post implantation.
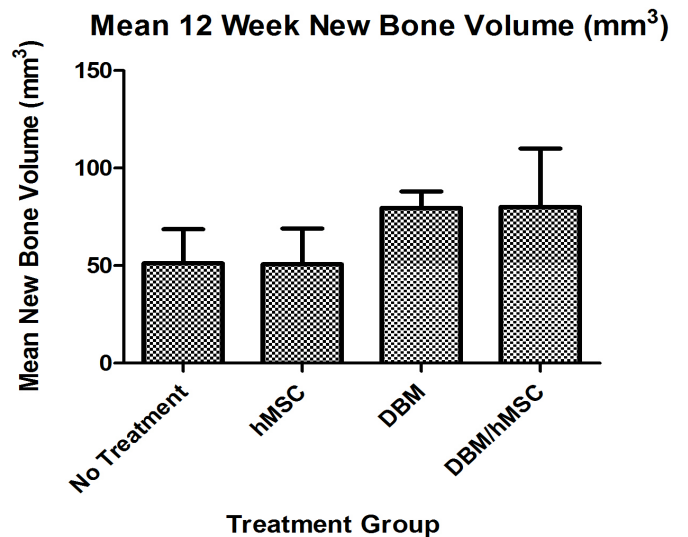
MicroCT

At 12 weeks, the DBM and the hMSC/ DBM treatment groups had the greatest new bone volume within the defects. Mean new bone volume was 79.6 mm^3 and 80.1 mm^3, respectively. The empty defect and the hMSC groups had less bone formation with mean values of 51.2 mm^3 and 50.7 mm^3, respectively. The 12 week µCT data are summarized in Figure 4.

Histological Analysis

There was minimal inflammation in noted in all treatment groups.

Empty Defect (No Treatment):

No bone formation was observed within histological sections of the empty defect group validating the 5 mm defect as a critical size defect in this experiment. Some active fibroplasia was observed with muscle collapse into the defect in 2 of the 3 sections evaluated for this treatment.

hMSC Group

The implant sites consisted of a marked amount of fibrosis admixed with a mild amount of neovascularization and a minimal number of macrophages. There were minimal numbers of multinucleated giant cells within the fibrosis of four of the five tissue sections. There was a mild amount of new trabecular (lamellar) and woven bone and a minimal amount of new cartilage within the edges of the bone on both sides of the implant site.

DBM Group

The implant sites consisted of a mild amount of anuclear demineralized bone material surrounded and divided by a mild amount of new trabecular (lamellar) bone, a mild to moderate amount of new woven bone, and a minimal amount of new cartilage. There were variably sized pockets of new bone marrow. Also admixed within the tissue reaction of the implant sites were a minimal to mild
amount of fibrosis, a mild to moderate amount of neovascularization, and a minimal number of macrophages and multinucleated giant cells. The new bone and cartilage growth was moderately bridging the implant sites.

hMSC/DBM Group

The implant sites consisted of a mild to moderate amount of anuclear demineralized bone material markedly surrounded and divided by a mild amount of new trabecular (lamellar) bone, a mild to moderate amount of new woven bone, and a minimal amount of new cartilage. There were variably sized pockets of new bone marrow surrounded by the new bone. Also admixed within

the tissue reaction of the implant sites was a minimal to mild amount of fibrosis, and a minimal to moderate amount of neovascularization. There were minimal numbers of macrophages and multinucleated giant cells in the tissue reaction of three of the implant sites; and minimal amount of polymorphonuclear cells in the tissue reaction of one of the implant sites. The new bone and cartilage growth was mildly to fully bridging the implant sites.

3.4 Comparison with Rat and Human Cortico-cancellous Bone Graft

Radiographic Analysis:

Appropriate alignment and fixation were maintained throughout the study term. Mineralized implanted material could be seen immediately after surgery on radiographs in the defects treated with rat and human corticocancellous bone, whereas no mineralized material could be seen in defects treated with DBM/hMSC. However, by 42 days post-implantation, bony union across the critical-sized femur defect was radiographically present in 2/3 defects treated with DBM/hMSC, 0/3 defects treated with rat-derived cortico-cancellous graft and 0/3 defects with human-derived cortico-cancellous bone (Figure 5A-C).

Figure 5A Appearance of defect at 42 days following implantation of rat-derived fresh frozen cortico-cancellous isograft. Note the lack of union.

Figure 5B Appearance of defect at 42 days following implantation of human-derived fresh frozen cortico-cancellous allograft.

Figure 5C Appearance of defect at 42 days following implantation of DBM/hMSC. Note that there is union in this critical-sized femur defect at 42 days.

Figure 6: Mean bone volume within defects as measured on μCT analysis in defects treated with rat-derived cortico- cancellous graft (Rat C-C), DBM/hMSC (hMSC/DBM), and human-derived cortico-cancellous graft (human C-C)

MicroCT Analysis:

The mean bone volume within the defects as measured on microCT analysis was as follows for each treatment group: DBM/hMSC= 642.67 mm^3, rat-derived cortico- cancellous graft = 433.67 mm^3 and human-derived cortico-cancellous graft= 397.67 mm^3. These data are summarized in Figure 6.

Histology/Histomorphometry:

Mean percentage new bone formation as calculated from histological sections was as follows for each treatment group: rat-derived cortico-cancellous graft =12.65+/- 15.67, DBM/hMSC= 16.44+/-9.24 and human – derived cortico-cancellous graft =5.39 +/- 6.26. New bone formation was noted to occur along remaining demineralized bone fragments in the DBM/hMSC groups and between bone fragments in the human and rat corticocancellous bone.

Discussion:

Optimized MSC-bone graft substitute combination have enormous potential for augmentation of bone repair in severe trauma and other disease states where normal bone healing is compromised.[1] [10] To date, there is no single scaffold that is considered optimal for MSC osteogenesis. Human DBM and allogeneic MSCs have separately been shown to have biologic activity *in vivo*,[10-12] and both adipose-derived MSCs and DBM can be obtained in abundant amounts from human tissue donors. Given the availability of these tissues and their osteogenic activity, we endeavored to explore the possible synergistic activity of the combination of non-culture expanded MSCs derived from adipose with demineralized bone. The results of these pilot studies show clear evidence of potent osteogenic activity of the DBM/hMSC combination. Interestingly, the combination of DBM and hMSC has greater bone forming activity than either component alone. Of particular interest is the finding that hMSCs alone (without DBM scaffold) have little to no osteogenic activity when placed in either ectopic or orthotopic sites. This is consistent with findings from other investigators who have shown that the contribution of MSCs towards bone

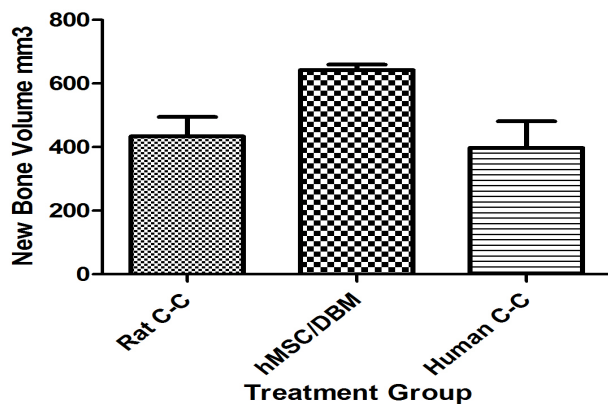formation requires the presence of a scaffold and/or osteoinductive proteins to heal bony voids.[5, 6, 10] Specifically researchers have demonstrated that MSC implanted on an inert carrier did not heal bone defects, but the combination of MSC plus the carrier plus bone morphogenic proteins led to complete or substantially improved healing. [13, 14 15,16, 17] *In vitro*, adipose derived MSCs have been demonstrated to require a signal to form bone. MSC without osteopromotive media remain in an undifferentiated state, whereas MSC plus dexamethasone or bone morphogenic protein does lead to bone formation.[18 19-21] The study highlights several parameters important for optimizing MSC contribution to bone formation. MSCs should be implanted with the optimal bone graft substitute, preferably one that contains the appropriate osteoinductive signals, such as DBM, rather than a scaffold, which lacks such a signal, such as a ceramic.

These data suggest that the bone formation activity resulting from implantation of DBM/hMSC is enhanced as compared to DBM alone. This was evidenced in several of the above pilot studies by a higher number of unions in critical-sized femur defects, greater new bone area on quantitative radiographic analysis and greater new bone volume on uCT analysis in the DBM/hMSC group as compared with the DBM alone groups.Thus, while DBM does contain osteoinductive proteins as previously described (8), added MSCs may respond to bone morphogenic protiens and other signals on the scaffold resulting in enhanced bone formation *in vivo*.

The studies using rat or human cortico-cancellous (C-C) bone were intended to compare bone formation properties between DBM/hMSC and autograft surrogates, since autograft is considered the gold standard. Although the C-C grafts were radio-opaque at the time of implantation, and DBM/hMSC was radiolucent, by six weeks greater new bone formation and radio-opacity for the DBM/hMSC treatment was observed as compared to the DBM implant as assessed by both uCT and histological assessments.

One unique characteristic of this study was that the MSCs were not proliferated *ex vivo* on tissue culture plastic and were not exposed to osteopromotive media prior to implantation. A number of publications utilized MSCs manipulated ex vivo prior to implantation to the bone defect.[22-24] Notable differences in MSCs have been observed during culture expansion of MSCs including the presence of chromosomal abnormalities, which lead to tumorigenicity concerns.[4, 7, 25] Also, ex vivo expansion methods are typically utilized to increase the number of bone contributing cells from tissue sources that have sub-efficacious amounts of MSCs (e.g. bone marrow).[26] These studies demonstrate that approximately 50,000 hMSC/cc was routinely obtained from human adipose donors in the absence of *ex vivo* cellular expansion and that this amount was sufficient to promote bone repair in this model.

These studies evaluated both acute short-term (6 week) and chronic long-term (12 week) outcomes. Acute evaluations were performed to determine the quantitative and qualitative effect of hMSC on early bone formation, whereas the chronic studies were performed to also assess the effect of hMSC on bone fusion.

The results that were obtained from the acute and the chronic studies cannot be directly compared since the studies were performed in different laboratories, different lots of graft material were utilized, and there were substantial differences in measurement methods, equipment and software. Similarly, comparison between the two acute studies cannot be directly compared.

The authors acknowledge the limitations of the small numbers of study subjects per individual experiment and because of this no statistical evaluation was performed. Nonetheless, the data support proof-of-efficacy and represent a body of evidence that, when taken together, paint a compelling picture of enhanced bone formation with DBM/hMSC. Confirmatory studies with adequate statistical power are currently underway in small animals.

4. Conclusion:

These studies have demonstrated the synergistic bone forming potential of DBM/hMSC in a variety of rigorous preclinical animal models. Together, the data support proof-of-concept that

DBM/hMSC will enhance bone formation in challenging healing environments.

References:

1.   Law S, Chaudhuri S. Mesenchymal stem cell and regenerative medicine: regeneration versus immunomodulatory challenges. American journal of stem cells 2013;2:22-38.

2.   Ra JC, Shin IS, Kim SH, et al. Safety of intravenous infusion of human adipose tissue-derived mesenchymal stem cells in animals and humans. Stem cells and development 2011;20:1297-1308.

3.   Radtke CL, Nino-Fong R, Esparza Gonzalez BP, Stryhn H, McDuffee LA. Characterization and osteogenic potential of equine muscle tissue- and periosteal tissue-derived mesenchymal stem cells in comparison with bone marrow- and adipose tissue-derived mesenchymal stem cells. American journal of veterinary research 2013;74:790- 800.

4.   Ben-David U, Mayshar Y, Benvenisty N. Large-scale analysis reveals acquisition of lineage-specific chromosomal aberrations in human adult stem cells. Cell stem cell 2011;9:97-102.

5.   Di Bella C, Aldini NN, Lucarelli E, et al. Osteogenic protein-1 associated with mesenchymal stem cells promote bone allograft integration. Tissue engineering Part A 2010;16:2967-2976.

6.   Jo CH, Yoon PW, Kim H, Kang KS, Yoon KS. Comparative evaluation of in vivo osteogenic differentiation of fetal and adult mesenchymal stem cell in rat critical-sized femoral defect model. Cell and tissue research 2013.

7.   Bochkov NP, Voronina ES, Katosova LD, Kuleshov NP, Nikitina VA, Chausheva AI. [Genetic safety of cellular therapy]. Vestnik Rossiiskoi akademii meditsinskikh nauk / Rossiiskaia akademiia meditsinskikh nauk 2011:5-10.

8.   Goldring CE, Duffy PA, Benvenisty N, et al.

9.   Assessing the safety of stem cell therapeutics. Cell stem cell 2011;8:618-628.

10.   Shi Y, Niedzinski JR, Samaniego A, Bogdansky S, Atkinson BL. Adipose- derived stem cells combined with a demineralized cancellous bone substrate for bone regeneration. Tissue engineering Part A 2012;18:1313-1321.

11.   Xu JZ, Qin H, Wang XQ, et al. Repair of large segmental bone defects using bone marrow stromal cells with demineralized bone matrix. Orthopaedic surgery 2009;1:34- 41.

12.   Clokie CM, Moghadam H, Jackson MT, Sandor GK. Closure of critical sized defects with allogenic and alloplastic bone substitutes. The Journal of craniofacial surgery 2002;13:111-121; discussion 122-113.

13.   Yew TL, Huang TF, Ma HL, et al. Scale-up of MSC under hypoxic conditions for allogeneic transplantation and enhancing bony regeneration in a rabbit calvarial defect model. Journal of orthopaedic research : official publication of the Orthopaedic Research Society 2012;30:1213-1220.

14.   Peterson B, Zhang J, Iglesias R, et al. Healing of critically sized femoral defects, using genetically modified mesenchymal stem cells from human adipose tissue. Tissue engineering 2005;11:120-129.

15.   Park KH, Kim H, Moon S, Na K. Bone morphogenic protein-2 (BMP-2) loaded nanoparticles mixed with human mesenchymal stem cell in fibrin hydrogel for bone tissue engineering. Journal of bioscience and bioengineering 2009;108:530-537.

16.   Kim HJ, Kim UJ, Kim HS, et al. Bone tissue engineering with premineralized silk scaffolds. Bone 2008;42:1226-1234.

17.   Kim SE, Jeon O, Lee JB, et al. Enhancement of ectopic bone formation by bone morphogenetic protein-2 delivery using heparin-conjugated PLGA nanoparticles with transplantation of bone marrow-derived mesenchymal stem cells. Journal of biomedical science 2008;15:771-777.

18.   Supronowicz P, Gill E, Trujillo A, et al. Human adipose-derived side population stem cells cultured on demineralized bone matrix for bone tissue engineering. Tissue engineering Part A 2011;17:789-798.

19.   Lin Y, Liu L, Li Z, et al. Pluripotency potential of human adipose-derived stem cells marked with exogenous green fluorescent protein. Molecular and cellular biochemistry 2006;291:1-10.

20.   Hsu WK, Wang JC, Liu NQ, et al. Stem cells from human fat as cellular delivery vehicles in an athymic rat posterolateral spine fusion model. The Journal of bone and joint surgery American volume 2008;90:1043-1052.

21.   Minamide A, Yoshida M, Kawakami M, et al. The effects of bone morphogenetic protein and basic fibroblast growth factor on cultured mesenchymal stem cells for spine fusion. Spine

2007;32:1067-1071.

22.   de Girolamo L, Arrigoni E, Stanco D, et al. Role of autologous rabbit adipose- derived stem cells in the early phases of the repairing process of critical bone defects. Journal of orthopaedic research : official publication of the Orthopaedic Research Society 2011;29:100-108.

23.   Lopez MJ, McIntosh KR, Spencer ND, et al. Acceleration of spinal fusion using syngeneic and allogeneic adult adipose derived stem cells in a rat model. Journal of orthopaedic research : official publication of the Orthopaedic Research Society 2009;27:366-373.

24.   Arinzeh TL, Peter SJ, Archambault MP, et al. Allogeneic mesenchymal stem cells regenerate bone in a critical-sized canine segmental defect. The Journal of bone and joint surgery American volume 2003;85-A:1927-1935.

25.   Shih HN, Shih LY, Sung TH, Chang YC. Restoration of bone defect and enhancement of bone ingrowth using partially demineralized bone matrix and marrow stromal cells. Journal of orthopaedic research : official publication of the Orthopaedic Research Society 2005;23:1293-1299.

26.   Nikitina VA, Osipova EY, Katosova LD, et al. Study of genetic stability of human bone marrow multipotent mesenchymal stromal cells. Bulletin of experimental biology and medicine 2011;150:627-631.

27.   Hernigou P, Poignard A, Beaujean F, Rouard H. Percutaneous autologous bone- marrow grafting for nonunions. Influence of the number and concentration of progenitor cells. The Journal of bone and joint surgery American volume 2005;87:1430-1437